



**QUEEN'S  
UNIVERSITY  
BELFAST**

## **Induction and antagonism of antiviral responses in respiratory syncytial virus-infected pediatric airway epithelium.**

Villenave, R., Broadbent, L., Douglas, I., Lyons, J. D., Coyle, P. V., Teng, M. N., Tripp, R. A., Heaney, L. G., Shields, M. D., & Power, U. F. (2015). Induction and antagonism of antiviral responses in respiratory syncytial virus-infected pediatric airway epithelium. *Journal of Virology*, *89*(24), 12309-12318.  
<https://doi.org/10.1128/JVI.02119-15>, <https://doi.org/10.1128/JVI.02119-15>

**Published in:**  
Journal of Virology

**Document Version:**  
Peer reviewed version

**Queen's University Belfast - Research Portal:**  
[Link to publication record in Queen's University Belfast Research Portal](#)

**Publisher rights**  
Copyright © 2015, American Society for Microbiology. All Rights Reserved.

**General rights**  
Copyright for the publications made accessible via the Queen's University Belfast Research Portal is retained by the author(s) and / or other copyright owners and it is a condition of accessing these publications that users recognise and abide by the legal requirements associated with these rights.

**Take down policy**  
The Research Portal is Queen's institutional repository that provides access to Queen's research output. Every effort has been made to ensure that content in the Research Portal does not infringe any person's rights, or applicable UK laws. If you discover content in the Research Portal that you believe breaches copyright or violates any law, please contact [openaccess@qub.ac.uk](mailto:openaccess@qub.ac.uk).

1 **Induction and antagonism of antiviral responses in respiratory syncytial virus-infected**  
2 **pediatric airway epithelium.**

3 Rémi Villenave<sup>+1\*</sup>, Lindsay Broadbent<sup>+1</sup>, Isobel Douglas<sup>2</sup>, Jeremy D. Lyons<sup>2</sup>, Peter V. Coyle<sup>3</sup>,  
4 Michael N. Teng<sup>4</sup>, Ralph A. Tripp<sup>5</sup>, Liam G. Heaney<sup>1</sup>, Michael D. Shields<sup>1,2</sup>, Ultan F. Power<sup>1#</sup>

5 <sup>1</sup>Centre for Infection & Immunity, School of Medicine, Dentistry & Biomedical Sciences, Queens  
6 University Belfast, Belfast BT9 7BL, Northern Ireland; <sup>2</sup>The Royal Belfast Hospital for Sick  
7 Children, Belfast BT12 6BA, Northern Ireland and <sup>3</sup>The Regional Virus Laboratory, Belfast Trust,  
8 Belfast, Belfast BT12 6BA, Northern Ireland; <sup>4</sup>Joy McCann Culverhouse Airway Disease Research  
9 Center, Department of Internal Medicine, University of South Florida Morsani College of  
10 Medicine, Tampa, FL 33647, USA; <sup>5</sup>Department of Infectious Diseases, University of Georgia,  
11 Athens, GA 30602, USA. \*Current address: Wyss Institute for Biologically Inspired Engineering,  
12 Harvard University, Boston, MA 02215, USA.

13 <sup>†</sup>These authors contributed equally to this paper.

14 **# Corresponding author:** Ultan F. Power- Tel: 44.28.9097.2285- [u.power@qub.ac.uk](mailto:u.power@qub.ac.uk)

15 **Research article**

16 **Running title (50 characters):** RSV and innate immunity in human airway epithelium

17 **Abstract word count:** 222

18 **Text word count:** 4139

19

20

## 21 **Abstract**

22 Airway epithelium is the primary target of many respiratory viruses. However, virus induction and  
23 antagonism of host responses by human airway epithelium remains poorly understood. To address  
24 this, we developed a model of respiratory syncytial virus (RSV) infection based on well-  
25 differentiated pediatric primary bronchial epithelial cell cultures (WD-PBECs) that mimics  
26 hallmarks of RSV disease in infants. RSV is the most important respiratory viral pathogen in young  
27 infants worldwide. We found that RSV induces a potent antiviral state in WD-PBECs that was  
28 mediated in part by secreted factors, including interferon lambda-1 (IFN $\lambda$ 1)/IL-29. In contrast, type  
29 I interferons were not detected following RSV infection of WD-PBECs., Interferon (IFN)  
30 responses in RSV-infected WD-PBECs reflected those in lower airway samples from RSV-  
31 hospitalized infants. In view of the prominence of IL-29, we determined whether recombinant IL-  
32 29 treatment of WD-PBECs before or after infection abrogated RSV replication. Interestingly, IL-  
33 29 demonstrated prophylactic, but not therapeutic, potential against RSV. The absence of  
34 therapeutic potential reflected effective RSV antagonism of IFN-mediated antiviral responses in  
35 infected cells. Our data are consistent with RSV non-structural proteins 1 and/or 2 perturbing the  
36 Jak-STAT signaling pathway, with concomitant reduced expression of antiviral effector molecules,  
37 such as MxA/B. Antagonism of Jak-STAT signaling was restricted to RSV-infected cells in WD-  
38 PBEC cultures. Importantly, our study provides the rationale to further explore IL-29 as a novel  
39 RSV prophylactic.

## 40 **Importance**

41 Most respiratory viruses target airway epithelium for infection and replication, which is central to  
42 causing disease. However, for most human viruses we have a poor understanding of their

43 interactions with human airway epithelium. Respiratory syncytial virus (RSV) is the most  
44 important viral pathogen of young infants. To help understand RSV interactions with pediatric  
45 airway epithelium, we previously developed 3-D primary cell cultures from infant bronchial  
46 epithelium that reproduce several hallmarks of RSV infection in infants, indicating that they  
47 represent authentic surrogates of RSV infection in infants. We found that RSV induced a potent  
48 antiviral state in these cultures and that type III interferon (IL-29) was involved. Indeed, our data  
49 suggest that IL-29 has potential to prevent RSV disease. However, we also demonstrated that RSV  
50 efficiently circumvents this antiviral immune response and identified mechanisms by which this  
51 may occur. Our study provides new insights into RSV interaction with pediatric airway epithelium.

52

### 53 **Introduction**

54 Airway epithelium is an extremely important barrier to respiratory pathogens. It is also the primary  
55 infection target for many respiratory viruses. Elucidating the interactions between respiratory  
56 viruses and airway epithelium is fundamental to understanding aspects of their pathogenesis. We  
57 recently developed and characterized models of respiratory syncytial virus (RSV) infection based  
58 on well-differentiated pediatric primary airway epithelial cells derived from pediatric bronchial  
59 (WD-PBECs) or nasal (WD-PNECs) brushings (1, 2). RSV is the primary viral cause of infant  
60 hospitalizations in the first year of life and is capable of repeated infections throughout life (3).  
61 Despite its original isolation in 1957 (4), no effective RSV therapies or vaccines are available. The  
62 mechanisms by which RSV causes disease and is capable of repeated infections in humans remain  
63 an enigma. Our models reproduce several hallmarks of RSV infection *in vivo*, suggesting that they

64 provide authentic surrogates with which to study RSV-induced innate immune responses and  
65 interaction with human airway epithelium (1, 2).

66 We previously reported secretion of high levels of CXCL10, an interferon-stimulated gene (ISG)  
67 product, from RSV-infected WD-PBECs (1, 2). This is consistent with the induction of an  
68 interferon (IFN)-mediated antiviral response to infection. IFNs are a heterogeneous family of  
69 cytokines with well characterized capacities to induce antiviral states in cells (5–7). They include  
70 types I (IFN- $\alpha/\beta$ ), II (IFN $\gamma$ ) and III (IFN $\lambda$ s), only the first and last of which are expressed by airway  
71 epithelial cells upon appropriate stimulation (8–10). Despite considerable CXCL10 secretion, we  
72 detected no IFN- $\alpha/\beta$  secretion from RSV-infected WD-PBECs, while little or no IFN- $\alpha/\beta$  was  
73 detected in nasal or bronchoalveolar lavages from RSV-infected infants (1, 2, 11–13). In contrast,  
74 little is known about IFN $\lambda$ s responses to RSV infection of airway epithelium *in vitro* and especially  
75 *in vivo*. IFN $\lambda$ s comprise three closely related molecules designated IFN $\lambda$ 1 (IL-29), IFN $\lambda$ 2 (IL-28A)  
76 and IFN $\lambda$ 3 (IL-28B) (IFN $\lambda$ 2 and 3 share 96% identity) (14). They are induced by viruses, such as  
77 influenza A virus and rhinovirus, and inhibit replication of HCV and HIV. Interestingly, we and  
78 others recently demonstrated that IFN $\lambda$ s, rather than IFN- $\alpha/\beta$ , were induced following RSV  
79 infection of primary monolayer or well-differentiated nasal and bronchial epithelial cell cultures  
80 (2, 15). This suggested a role for IFN $\lambda$ s in RSV-induced antiviral responses. IFN $\lambda$ s induce antiviral  
81 states by signaling through a heterodimeric receptor complex composed of IL-28R $\alpha$  and IL-10RA  
82 (14). This activates signal transduction through the Jak/STAT pathway in a manner that is virtually  
83 identical to IFN- $\alpha/\beta$ , resulting in phosphorylation of mainly signal transducer and activator of  
84 transcription (STAT)1 (pSTAT1) and STAT2 (pSTAT2) and, to a lesser extent, STAT3, 4 and 5.  
85 This is followed by pSTAT homo- or heterodimerisation, complexing with interferon regulatory

86 factor 9 (IRF9), nuclear translocation and induction of numerous ISGs, such as CXCL10 or the  
87 potent antiviral protein MxA (14, 16–18).

88 In the current study, we explored the induction of antiviral responses following RSV infection of  
89 WD-PBECs. We found that RSV induced a potent antiviral state against the related Sendai virus  
90 (SeV), which was mediated, in part at least, by secreted factors including IFN $\lambda$ 1/IL-29. We also  
91 demonstrated that RSV-induced IL-29 secretion from WD-PBECs reflected IL-29 secretions in  
92 lower airway samples from RSV-infected infants. These RSV-induced secreted factors also  
93 demonstrated prophylactic antiviral activity against RSV, albeit with lower potency than against  
94 SeV. Pre-treatment of WD-PBEC cultures with a high dose of IL-29 reduced RSV replication,  
95 suggesting the prophylactic potential of IL-29. Interestingly, RSV non-structural proteins NS1 and  
96 NS2, which we and others have previously shown to antagonize IFN- $\alpha$ / $\beta$ -mediated antiviral  
97 responses (19–21), were critical for RSV growth in WD-PBECs and antagonism of IL-29-induced  
98 antiviral responses. We also found that in WD-PBECs, RSV-infected cells had significantly  
99 reduced MxA/B and pSTAT2 expression levels compared to surrounding non-infected cells,  
100 indicating active antagonism of antiviral responses by RSV but restriction of this antagonism to  
101 infected cells. In summary, our data provide novel insights into the induction and antagonism of  
102 antiviral responses, and in particular IL-29, following RSV infection of human airway epithelium.

103

#### 104 **Material and Methods.**

105 **Cell lines and viruses.** HEp-2 and Vero cell lines were cultured as previously described (22). The  
106 origin and characterization of the clinical isolate RSV BT2a were previously described (23).  
107 Recombinant RSV expressing eGFP (rA2-eGFP) was generated by cloning a cassette consisting of

108 the eGFP ORF-NS1 gene end signal-NS1 gene start signal into an antigenomic cDNA (D53) of  
109 RSV at the position of the NS1 ATG. This scheme inserts an additional transcription unit encoding  
110 eGFP at the first position in the genome, preserving the RSV sequence from the leader through the  
111 NS1 5' UTR. The eGFP containing D53 was then used to recover recombinant RSV in BSR-T7  
112 cells as described (20, 24, 25). Production of recombinant RSV expressing eGFP in place of NS1  
113 and NS2 (rA2- $\Delta$ NS1/2-eGFP) has been described (26). rA2-eGFP and rA2- $\Delta$ NS1/2-eGFP stock  
114 production and titrations were performed in Vero cells. Virus stocks were harvested and stored as  
115 previously described (27). Rescue, characterization, stock production and titration of rSeV/eGFP  
116 were previously described (22).

117 **WD-PBEC culture and infection.** WD-PBEC culture was described previously (28). Briefly,  
118 primary pediatric bronchial epithelial cells were obtained by bronchial brushings from healthy  
119 children undergoing elective surgery, expanded in culture flasks and seeded onto collagen-coated  
120 Transwell inserts (6.5 mm diameter, 0.4  $\mu$ m pore size). Once confluence was reached, apical  
121 medium was removed to create an air-liquid interface (ALI) and trigger differentiation into pseudo-  
122 stratified mucociliary epithelium. Cultures were infected 3 to 4 weeks after ALI, as previously  
123 described (28), with multiplicities of infection (MOI) specified in the Figure legends. Virus stocks  
124 were diluted in DMEM where necessary. Inoculum or DMEM-only were added to the apical  
125 surface and cultures were incubated for 1.5 h at 37°C in 5% CO<sub>2</sub> followed by 5 rinses with 500  $\mu$ l  
126 DMEM. The last rinse was retained as the 2 h virus titration point. Every 24 h thereafter, apical  
127 rinses and basal medium were collected to determine virus growth kinetics and IFN responses,  
128 respectively. Infected and control cultures were monitored daily by light and UV microscopy,  
129 where appropriate (Nikon Eclipse TE-2000U). eGFP quantification in infected cultures was  
130 performed using ImageJ software (<http://rsbweb.nih.gov/ij/>).

131 **Immunofluorescence, ELISA.** Immunostaining of the cultures was previously described (28).  
132 Briefly, WD-PBECs were rinsed with PBS and fixed with 4% paraformaldehyde for 20 min.  
133 Cultures were washed and stored in PBS at 4°C until used. For immunofluorescence staining,  
134 cultures were permeabilized with PBS plus 0.2% Triton X-100 (v/v) for 2 h and blocked with 0.4%  
135 BSA (w/v) in PBS for 30 min. RSV-infected cells were detected using an anti-RSV F-specific  
136 mouse monoclonal antibody (MAb) (clone 133-1H conjugated with ALEXA 488,  
137 1:200, Chemicon, US). MxA/B was detected using an anti-human Mx mouse MAb (Santa-Cruz,  
138 clone C-1, 1:200). pSTAT1 and pSTAT2 were detected using mouse anti-human pSTAT1 (pY701)  
139 MAb (BD Biosciences, 1:200) and rabbit anti-human pSTAT2 (Tyr690) polyclonal antibody  
140 (Antibodies-online, Inc, GA, USA; 1:200), respectively. The mouse anti-Mx and pSTAT1 (pY701)  
141 MAbs were detected with ALEXA-568-conjugated goat anti-mouse IgG1 (Invitrogen, 1:500),  
142 while rabbit polyclonal antibodies were detected with ALEXA-568-conjugated goat anti-rabbit  
143 IgG (H+L) (Invitrogen, 1:500) polyclonal antibodies, respectively. Inserts were mounted on  
144 microscopy slides and nuclei were counterstained using DAPI mounting medium (Vectashield).  
145 Fluorescence was detected by confocal laser scanning microscopy (TCS SP5, LEICA). MX and p-  
146 STAT fluorescence intensities were determined using confocal images of infected cultures in  
147 ImageJ by dividing the Raw Integrated Density by the area of each individual cell. This was done  
148 for >120 RSV-infected and non-infected cells.

149 IL-29 (IFN- $\lambda$ 1), pan-IFN- $\alpha$  and IFN- $\beta$  concentrations in WD-PBEC basal media and in clinical  
150 samples were measured using human IFN- $\lambda$ 1 ELISA kits (eBioscience, UK), human IFN- $\beta$  ELISA  
151 kits (R&D Systems), and human pan-IFN- $\alpha$  ELISA kits (Mabtech, Sweden). All ELISAs were  
152 undertaken according to the manufacturers' instructions. IL-28A (IFN- $\lambda$ 2) was detected using a  
153 custom Milleplex kit, according to the manufacturer's instructions (Merck-Millipore, UK)



154 **Super-infection, conditioned medium and IFN- $\lambda$  treatment.** Super-infection experiments were  
155 undertaken by infecting WD-PBECs with RSV BT2a (MOI  $\approx$  4) for 72 h and super-infecting them  
156 with rSeV/eGFP (MOI  $\approx$  0.1), as described previously for 144 h (28). Conditioned medium (CM)  
157 experiments were performed by transferring basal medium from mock- (CM<sub>CON</sub>) or RSV-infected  
158 WD-PBECs cultures incubated with (CM<sub>RSV</sub> +  $\alpha$ IL-29) or without (CM<sub>RSV</sub>) neutralizing antibody  
159 against IL-29 (R&D systems – MAB15981 - 10  $\mu$ g/mL) at 72 hpi into the basal compartment of  
160 fresh cultures derived from the same individuals. Twenty four hours later conditioned cultures were  
161 infected with rSeV/eGFP. To assess anti-viral effects of IFN- $\lambda$ 1/IL-29 against RSV, rSeV/eGFP,  
162 rA2-eGFP and rA2- $\Delta$ NS1/2-eGFP, fresh WD-PBECs or Vero cells were treated before or after  
163 infection with IFN- $\lambda$ 1/IL-29 (Peprotech, UK). Antiviral effects were determined by measuring  
164 eGFP fluorescence and/or virus growth kinetics.

165 **Lower airway sampling.** Samples were obtained from 10 infants (mean age 0.31 years, range  
166 0.06 -1.3 years) with severe RSV disease who were treated in the pediatric intensive care unit of  
167 the Royal Belfast Hospital for Sick Children. Samples were direct tracheobronchial aspirates or  
168 deeper suction samples following the instillation of 2 mL saline. All sampling was clinically  
169 indicated and not performed for research purposes. Fourteen uninfected and otherwise healthy  
170 children (mean age 1.7 years, range 1-2.4 years) acted as controls with blind non-bronchoscopic  
171 bronchoalveolar lavage samples obtained (after instillation of 10 mL saline) at the time of  
172 intubation for an elective surgical procedure (29). All RSV-infected infants were confirmed as  
173 having mono-infections using a multiplex virus reverse transcriptase (RT)-PCR strip for 12  
174 respiratory viruses, as previously described (30).

175 **Statistical analyses.** Data obtained *in vitro* were described as mean [ $\pm$  SEM] and skewed data were  
176 log transformed before comparisons were made by Student's paired t-test or by comparing the areas

177 under the curves using GraphpadPrism<sup>®</sup> 5.0. Data from RSV-infected and control children were  
178 compared using a Mann-Whitney t-test using GraphpadPrism<sup>®</sup> 5.0.  $p < 0.05$  was considered  
179 statistically significant.

180 **Ethics.** This study was approved by The Office for Research Ethics Committees Northern Ireland  
181 (ORECNI). Written informed parental consent was obtained.

182

## 183 **Results**

### 184 **RSV infection induces an antiviral state in WD-PBECs.**

185 RSV infection of WD-PBECs generally occurred in non-contiguous or small clusters of ciliated  
186 epithelial cells (1, 2). This suggested the possibility that infection induced an anti-viral state in  
187 neighboring non-infected cells that limited viral spread. To detect the induction of antiviral  
188 responses we used rSeV/eGFP, as SeV replicates efficiently in WD-PBECs but is restricted in  
189 human cells pre-treated with human IFN (22, 28, 31). WD-PBECs (n=3 donors) were mock-  
190 infected or infected with RSV BT2a (MOI~4). Seventy-two h later, the cultures were super-infected  
191 with rSeV/eGFP (MOI~0.1). Fluorescence was monitored and apical washes were collected for  
192 virus titration every 24 h post-infection (hpi) with rSeV/eGFP for 144 h. Pre-infection with RSV  
193 potently inhibited rSeV/eGFP replication, as evidenced by greatly diminished eGFP expression  
194 and rSeV/eGFP growth kinetics (Fig. 1A-C). Thus, RSV infection induced a strong antiviral state  
195 in WD-PBECs.

### 196 **IFN $\lambda$ 1/IL-29 is the predominant interferon following RSV infection *in-vivo* and *in-vitro*.**

197 Previous work from us and others reported little or no IFN- $\alpha/\beta$  secretion following RSV infection  
198 of infants or airway epithelial cells *in vitro* (1, 32). In contrast, IL-29 was evident following RSV  
199 infection of primary airway (nasal) epithelial cells *in vitro* (2, 15). To confirm and extend these  
200 findings, we determined IFN- $\alpha/\beta$ , IL-28A and IL-29 concentrations in lower airway samples from  
201 infants hospitalized with severe RSV (n=8-10) and uninfected controls (n=11-14). Apart from one  
202 RSV-infected individual with low levels of IFN $\alpha$ , no IFN- $\alpha/\beta$  was detected in lower airway samples  
203 from infected infants (Fig. 2A and B). In contrast, IL-29 was significantly elevated in lower airway  
204 samples from RSV-infected patients compared to controls (Fig. 2C), although IL-28A was not (Fig.  
205 2D). Furthermore, IL-29 concentrations in basolateral medium from RSV-infected WD-PBECs  
206 were significantly increased compared to controls and were similar to those in lower airway  
207 samples (Fig. 2E). Thus, our RSV/WD-PBEC model reproduced IL-29 responses to RSV infection  
208 *in-vivo*. Similarly, CM<sub>RSV</sub> from 2/5 RSV-infected WD-PBECs had only low levels of IL-28A at  
209 96 hpi (Fig. 2F). The cumulative data suggest that IL-29 is an important IFN protagonist induced  
210 by RSV infection of infants and WD-PBECs and consequently might be responsible for the RSV-  
211 induced antiviral responses. Whether IFN- $\alpha/\beta$  are implicated in these antiviral responses, in  
212 contrast, is unlikely, although this remains to be definitively confirmed.

### 213 **Secreted factors, including IL-29, are implicated in the RSV-induced antiviral state.**

214 To determine if secreted factors, including IL-29, were implicated in the antiviral state induced in  
215 RSV-infected WD-PBECs, cultures (n=2-3 donors) were mock-infected or infected with RSV  
216 BT2a (MOI~1 or 4). At 72 hpi, CM<sub>RSV</sub> (with or without anti-IL-29 – 10  $\mu$ g/mL) and CM<sub>CON</sub> were  
217 transferred to uninfected cultures derived from the same individuals. The cultures were infected 24  
218 h later with rSeV/eGFP (MOI~0.1). eGFP expression (Fig. 3A, B) and rSeV/eGFP growth kinetics  
219 (Fig. 3C) indicated that factors secreted from RSV BT2a-infected WD-PBECs were responsible,

220 in part, for the RSV-induced antiviral effects. Importantly, when  $CM_{RSV}$  was pre-incubated with  
221 anti-IL-29 ( $CM_{RSV} + \alpha IL-29$ ), the ability of  $CM_{RSV}$  to abrogate rSeV/eGFP infection was  
222 significantly reduced, suggesting an important role for IL-29 in the antiviral effect of  $CM_{RSV}$ .

### 223 **IL-29 attenuates rSeV/eGFP replication in WD-PBECs.**

224 To confirm that IL-29 has antiviral activities in airway epithelium, WD-PBECs (n=2-3 donors)  
225 were pre-treated for 24 h with 100 or 1000 pg/mL IL-29 before infecting with rSeV/eGFP  
226 (MOI~0.1). These concentrations represented high physiological and super-physiological  
227 concentrations of IL-29, respectively, relative to IL-29 concentrations evident in  $CM_{RSV}$  and lower  
228 airway samples. IL-29 demonstrated a dose-dependent suppression of eGFP expression following  
229 rSeV/eGFP infection, although both doses resulted in substantial reductions in eGFP expression  
230 relative to controls (Fig. 4A, B). Furthermore, rSeV/eGFP growth kinetics were significantly  
231 reduced following pre-treatment with both IL-29 doses (Fig. 4C), although these reductions, even  
232 at the higher dose, were lower than those evident after  $CM_{RSV}$  pre-treatment (Fig. 3C). The data  
233 demonstrated that IL-29 has antiviral activities in airway epithelium and may account for some,  
234 but not all, of the antiviral activity associated with  $CM_{RSV}$ .

### 235 **$CM_{RSV}$ and IL-29 prophylaxis attenuates RSV growth in WD-PBECs.**

236 To assess  $CM_{RSV}$  antiviral activity against RSV, WD-PBECs cultures (n=2 donors) were mock-  
237 infected or infected with RSV BT2a (MOI~4). At 72 hpi,  $CM_{CON}$  and  $CM_{RSV}$  were transferred to  
238 uninfected cultures derived from the same individuals.  $CM$ -treated cultures were infected with rA2-  
239 eGFP (MOI~0.1) 24 h later and fluorescence was monitored for 96 h (Fig. 5A). The eGFP  
240 expression data demonstrated a similar, albeit lower, antiviral effect of  $CM_{RSV}$  against RSV

241 compared with rSeV/eGFP (Fig. 5A). This was also reflected in significantly reduced rA2-eGFP  
242 growth kinetics in CM<sub>RSV</sub>-treated compared to CM<sub>CON</sub>-treated WD-PBEC cultures (Fig. 5B).

243 To assess whether IL-29 had prophylactic or therapeutic potential against the clinical isolate RSV  
244 BT2a, cultures (n=3 donors) were untreated or treated with IL-29 for 24 h before infection  
245 (MOI~0.01) (1 ng/mL or 100 ng/mL), or at 2 or 24 hpi (100 ng/mL). Pre-treatment with 100 ng/mL  
246 IL-29 significantly reduced RSV replication (p<0.05), while pre-treatment with 1 ng/mL IL-29 did  
247 not (Fig. 5C). In contrast, IL-29 did not demonstrate therapeutic potential against RSV under our  
248 experimental conditions (Fig. 5D). The cumulative data from Figs. 3 and 5 suggested that RSV is  
249 more resistant to CM<sub>RSV</sub> and IL-29 than rSeV/eGFP, and that the antiviral activity of CM<sub>RSV</sub>  
250 against RSV in WD-PBECs is similar to that evident following pre-treatment with 100 ng/mL IL-  
251 29. In view of the considerably lower levels of IL-29 evident in CM<sub>RSV</sub> than those used in these  
252 experiments, IL-29 is unlikely to be solely responsible for the limited spread of RSV in WD-  
253 PBECs.

#### 254 **RSV NS proteins antagonize IL-29-mediated anti-viral effects.**

255 The relative resistance of RSV to IL-29 suggested efficient antagonism of the IFN $\lambda$ -signaling  
256 pathway in WD-PBECs. We and others have shown that RSV NS1 and particularly NS2 are  
257 responsible for antagonizing IFN- $\alpha/\beta$  signaling through degradation of pSTAT2 (19, 33). However,  
258 the capacity of RSV NS1/2 to antagonize IFN $\lambda$ -mediated innate immune responses is unknown.  
259 To determine whether these proteins were implicated in antagonising IL-29-induced responses in  
260 WD-PBECs, cultures were initially infected with recombinant RSV expressing eGFP, either wild-  
261 type (rA2-eGFP) or lacking NS1 and NS2 (rA2- $\Delta$ NS1/2-eGFP) (MOI~0.1). While rA2-eGFP grew  
262 efficiently in WD-PBECs, replication of the NS1/2-deleted mutant was virtually abrogated (Fig.

263 6), indicating that NS1 and/or NS2 were critical for RSV replication in WD-PBECs. This result  
264 precluded the use of WD-PBECs to address antagonism of IL-29-mediated antiviral responses by  
265 RSV. As both the mutant and wild type viruses grew efficiently in Vero cells and these cells were  
266 sensitive to IFN $\lambda$ s stimulation (34, 35), we addressed the role of RSV NS1/2 in IL-29 antagonism  
267 in Vero cells. The cells were pre-treated with IL-29 (1 or 100 ng/ml) or mock-treated for 24 h  
268 before infection with either rA2-eGFP or rA2- $\Delta$ NS1/2-EGFP (MOI~0.1). Treated and control  
269 cultures were subsequently incubated for 72 h in the presence and absence of IL-29, respectively.  
270 Pre-treatment with 1 ng/mL IL-29 had no effect on rA2-eGFP replication, as indicated by eGFP  
271 expression kinetics, while 100 ng/mL did (Fig. 7A, C). By comparison, pre-treatment with either  
272 dose of IL-29 had much more dramatic effects on rA2- $\Delta$ NS1/2-eGFP replication than rA2-eGFP  
273 (Fig. 7B, D). Thus, RSV NS1/2 proteins are implicated in antagonizing IL-29-mediated antiviral  
274 responses.

#### 275 **RSV antagonizes pSTAT2 and MxA/B expression in WD-PBECs.**

276 To gain insight into the mechanisms behind RSV antagonism of the antiviral responses induced in  
277 WD-PBECs, we looked at the capacity of RSV to antagonize Jak/STAT signalling and MxA/B  
278 expression on a single cell basis within individual infected and surrounding non-infected cells. As  
279 MxA/B expression is a reliable marker of IFN bioactivity (36), we initially confirmed that RSV  
280 infection, IL-29 treatment, or CM<sub>RSV</sub> treatment induced MxA/B expression in WD-PBECs (Fig.  
281 8A and B). Furthermore, when CM<sub>RSV</sub> was pre-treated with anti-IL-29, MxA/B expression was  
282 virtually abrogated, demonstrating that MxA/B induction following CM<sub>RSV</sub>-treatment was in large  
283 part mediated by IL-29 (Fig. 8B and C). We and others previously reported that RSV NS proteins  
284 block the IFN $\alpha/\beta$ -stimulated Jak/STAT signalling pathway by targeting pSTAT2 for proteasomal  
285 degradation (19, 37). To study RSV antagonism of Jak/STAT signalling and MxA/B expression in

286 WD-PBECs, cultures (n=3-4 donors) were infected with RSV (MOI~0.1), subjected to daily apical  
287 rinses and basolateral medium change, fixed, permeabilized and co-stained for RSV F and either  
288 pSTAT1, pSTAT2 or MxA/B at 144 hpi (Fig. 9A-F). pSTAT1 fluorescence intensities were similar  
289 in both infected and non-infected cells (Fig. 9E, F). In contrast, pSTAT2 protein was significantly  
290 diminished (Fig. 9C, D), while MxA/B proteins were virtually absent (Fig. 9A, B), in RSV-infected  
291 compared to surrounding non-infected cells. Thus, antagonism of the RSV-induced IFN-mediated  
292 antiviral responses was restricted to infected cells and implicated the perturbation of the Jak/STAT  
293 signalling pathway by pSTAT2 down-regulation.

## 294 **Discussion**

295 Innate immune responses are critical first lines of defense against virus infection (38, 39). The  
296 capacity for viruses to antagonize or circumvent these responses is essential for their successful  
297 replication. Our RSV/WD-PBEC model provided a unique opportunity to study the induction and  
298 antagonism of innate antiviral immune responses by RSV in a morphologically- and  
299 physiologically-authentic model of pediatric bronchial epithelium. We exploited the fact that RSV  
300 infection does not lead to gross destruction of WD-PBECs to establish super-infection experiments  
301 with rSeV/eGFP. rSeV/eGFP was particularly useful for these experiments as it replicates very  
302 efficiently in untreated WD-PBECs but is sensitive to human IFN (28, 31). These characteristics  
303 provided the unique opportunity to establish a novel bioassay to study RSV-induced antiviral  
304 responses in WD-PBECs based on SeV-derived eGFP expression and SeV growth kinetics.

305 Our rSeV/eGFP super-infection bioassay unambiguously demonstrated that RSV induced a potent  
306 antiviral response in WD-PBECs and that basolaterally-secreted factors were, in part, responsible  
307 for this anti-viral activity. Importantly, IFN- $\lambda$ s, particularly IL-29, but not IFN- $\alpha/\beta$ , were detected

308 in RSV-infected WD-PBECs. This is consistent with Okabayashi *et al* (2011), who showed a  
309 predominance of IL-29 secretion from RSV-infected primary and immortalized nasal epithelial cell  
310 monolayers (15). A major finding of our study is the preponderance of IL-29 and the absence of  
311 detectable IFN- $\alpha/\beta$  in lower airway samples from RSV-infected infants, suggesting that IFN- $\lambda$ s,  
312 and in particular IL-29, are the principal interferons responding to RSV infection *in vitro* and *in*  
313 *vivo*. The lack of detectable IFN- $\alpha/\beta$  in CM<sub>RSV</sub>, as reported previously (1), and in lower airway  
314 samples from infants hospitalized with RSV, as reported here, is consistent with earlier clinical  
315 observations (11–13). It is unclear whether this lack of detectable IFN- $\alpha/\beta$  in CM<sub>RSV</sub> is due to a  
316 failure to stimulate these responses and/or active antagonism of induction by RSV NS1/2. Indeed,  
317 using immortalized cell lines, RSV NS proteins were shown to antagonize IFN $\alpha/\beta$  induction by  
318 interacting with RIG-I, disrupting association of IRF-3 with CBP and, thereby, IRF-3 binding to  
319 the IFN- $\beta$  promoter, and suppressing activation and nuclear translocation of IRF-3 (19, 40, 41)  
320 They also antagonized IFN $\alpha/\beta$  signaling by inducing proteasome-mediated degradation of pSTAT2  
321 (19, 37) . Additionally, RSV NS1, and to a lesser extent NS2, were shown to decrease cellular  
322 levels of TRAF3 and IKK $\epsilon$ , both key members of the IFN response pathway (42). However, Killip  
323 *et al* recently demonstrated that even when viral IFN $\alpha/\beta$  antagonists were deleted, the  
324 paramyxovirus PIV5 failed to activate the IFN $\beta$  promoter, suggesting that members of the  
325 *Paramyxoviridae* are very inefficient at inducing IFN- $\alpha/\beta$  responses (43). The corollary, however,  
326 is that the IFN antagonistic capacities of these viruses likely evolved to cope with IFN- $\lambda$ s, rather  
327 than IFN- $\alpha/\beta$ , responses.

328 Therefore, we evaluated the capacity of RSV NS1/2 to antagonize IFN- $\lambda$ 1/IL-29-mediated antiviral  
329 effects. We demonstrated that NS1 and/or NS2 were essential for RSV resistance to IL-29-  
330 mediated antiviral activity in Vero cells and for replication of RSV in WD-PBECs. At a cellular



331 level in WD-PBECs, we showed that RSV infection inhibited the interferon-inducible Jak/STAT  
332 pathway through p-STAT2 suppression, with concomitant reduction of the expression of the IFN-  
333 induced antiviral GTPases, MxA/B (18). However, this inhibition in WD-PBECs was restricted to  
334 infected cells. As MxA/B are reliable markers of IFN bioactivity and IL-29 was the only IFN  
335 detected in CM<sub>RSV</sub>, our cumulative data are consistent with a model in which RSV infection  
336 induces IL-29-mediated antiviral activity in WD-PBECs but that RSV NS1/2 proteins efficiently  
337 antagonize these responses only in infected cells through pSTAT2 degradation. Although IFN $\alpha/\beta$   
338 were not detected in our assays, the possibility remains that very low biologically active levels  
339 were present. Further work is therefore needed to definitively exclude their role in RSV-induced  
340 antiviral responses in WD-PBECs.

341 There is an increasing body of evidence confirming the capacity of IL-29 to induce antiviral states  
342 in infected cells (5, 8, 44). Our data extend this IL-29 capacity to SeV and RSV. We found no  
343 evidence that IL-29 has therapeutic potential against RSV infection. However, we present evidence  
344 that IL-29 has prophylactic potential against RSV, as demonstrated by retarded RSV growth  
345 kinetics in IL-29 pre-treated WD-PBECs compared with untreated controls. These data provide the  
346 rationale for further studies on IL-29 prophylaxis to modulate RSV pathogenesis. This is of  
347 particular interest for individuals at risk for severe illness due to RSV infection, although more  
348 work is needed to better understand IL-29 responses *in vivo*. Moreover, the IL-29-mediated  
349 antiviral effects against RSV, combined with the tissue-restriction of the type III IFN receptor to  
350 epithelial cells, the liver and some leukocytes suggest that IL-29 prophylaxis may result in limited  
351 toxicities that are typical of type I IFN therapy (45). Indeed, early data from clinical trials using  
352 IFN- $\lambda$  to treat chronic hepatitis C virus support this possibility (46).

353 Our evidence suggests the exciting prospect of potentially novel potent antiviral molecules in  
354 CM<sub>RSV</sub> that are not explained by its IL-29 content alone. Neutralizing IL-29 eliminated a large  
355 portion of the antiviral activity of CM<sub>RSV</sub>. However, CM<sub>RSV</sub> demonstrated greater antiviral potency  
356 than 1 ng/mL recombinant IL-29, which represents ~25 fold increase relative to the mean IL-29  
357 concentration in CM<sub>RSV</sub>. Therefore, it is possible that other molecules in CM<sub>RSV</sub> act in synergy  
358 with IL-29 to exert its impressive antiviral activities. Indeed, such synergistic antiviral activity was  
359 previously reported for IFN $\alpha/\beta$  and INF $\gamma$  against herpes simplex virus 1 (HSV-1), hepatitis C virus  
360 (HCV) and severe acute respiratory syndrome-associated coronavirus (SARS-CoV)(47–49).  
361 However, further work is required to identify such molecules and determine whether such synergy  
362 is evident in our WD-PBEC model.

363 Finally, there is increasing molecular diagnostic evidence demonstrating concomitant dual or  
364 multiple respiratory viral infections in individuals (50, 51). Debate is ongoing as to whether such  
365 dual/multi-infections result in exacerbated disease compared with mono-infections. Extrapolation  
366 of our data to the clinic suggests that a primary infection with RSV would result in the induction  
367 of an antiviral state in the airway epithelium that may greatly compromise the capacity of  
368 subsequent viruses to infect and replicate, unless the second virus was adept at circumventing the  
369 pre-established innate immune responses. This is consistent with a recent study showing that  
370 infection with multiple respiratory viruses correlated with less severe disease (52).

371 In conclusion, our study significantly advances our understanding of RSV induction and  
372 antagonism of type III IFN responses in human airway epithelium. Importantly, it provides the  
373 rationale for dissecting the molecular mechanisms by which these occur and the possible  
374 exploitation of IL-29 as a novel RSV prophylactic, either alone or in combination with other yet-  
375 to-be discovered CM<sub>RSV</sub> antiviral molecules.

376

377 **Acknowledgments**

378 We are most grateful to the children and parents who consented to participate in this study. Funding  
379 was provided by the Public Health Agency HSC Research & Development Division, Northern  
380 Ireland, the European Social Fund, Northern Ireland Chest Heart and Stroke, and the Royal Belfast  
381 Hospital for Sick Children. MNT thanks Peter Collins (NIAID) for the use of the RSV reverse  
382 genetics system.

383

384 **References**

- 385 1. **Villenave R, Thavagnanam S, Sarlang S, Parker J, Douglas I, Skibinski G, Heaney LG,**  
386 **McKaigue JP, Coyle P V, Shields MD, Power UF.** 2012. In vitro modeling of respiratory  
387 syncytial virus infection of pediatric bronchial epithelium, the primary target of infection in  
388 vivo. *Proc Natl Acad Sci U S A* **109**:5040–5.
- 389 2. **Guo-Parke H, Canning P, Douglas I, Villenave R, Heaney LG, Coyle P V, Lyons JD,**  
390 **Shields MD, Power UF.** 2013. Relative respiratory syncytial virus cytopathogenesis in  
391 upper and lower respiratory tract epithelium. *Am J Respir Crit Care Med* **188**:842–51.
- 392 3. **Glezen WP, Taber LH, Frank AL, Kasel JA.** 1986. Risk of primary infection and  
393 reinfection with respiratory syncytial virus. *Am J Dis Child* **140**:543–546.

- 394 4. **Chanock R, Roizman B, Myers R.** 1957. Recovery from infants with respiratory illness of  
395 a virus related to chimpanzee coryza agent (CCA). I. Isolation, properties and  
396 characterization. *Am J Hyg* **66**:281–90.
- 397 5. **Kotenko S V, Gallagher G, Baurin V V, Lewis-Antes A, Shen M, Shah NK, Langer JA,**  
398 **Sheikh F, Dickensheets H, Donnelly RP.** 2003. IFN-lambdas mediate antiviral protection  
399 through a distinct class II cytokine receptor complex. *Nat Immunol* **4**:69–77.
- 400 6. **Zorzitto J, Galligan CL, Ueng JJM, Fish EN.** 2006. Characterization of the antiviral  
401 effects of interferon-alpha against a SARS-like coronavirus infection in vitro. *Cell Res*  
402 **16**:220–9.
- 403 7. **Samuel CE.** 2001. Antiviral actions of interferons. *Clin Microbiol Rev* **14**:778–809.
- 404 8. **Ank N, West H, Bartholdy C, Eriksson K, Thomsen AR, Paludan SR.** 2006. Lambda  
405 interferon (IFN-lambda), a type III IFN, is induced by viruses and IFNs and displays potent  
406 antiviral activity against select virus infections in vivo. *J Virol* **80**:4501–9.
- 407 9. **Jewell N a, Cline T, Mertz SE, Smirnov S V, Flaño E, Schindler C, Grieves JL, Durbin**  
408 **RK, Kotenko S V, Durbin JE.** 2010. Lambda interferon is the predominant interferon  
409 induced by influenza a virus infection in vivo. *J Virol* **84**:11515–22.
- 410 10. **Jewell N a, Vaghefi N, Mertz SE, Akter P, Peebles RS, Bakaletz LO, Durbin RK, Flaño**  
411 **E, Durbin JE.** 2007. Differential type I interferon induction by respiratory syncytial virus  
412 and influenza a virus in vivo. *J Virol* **81**:9790–800.

- 413 11. **Hall CB, Jr RGD, Simons RL, Geiman JM.** 1978. Interferon production in children with  
414 respiratory syncytial, influenza, and parainfluenza virus infections. *J Pediatr* **93**:28–32.
- 415 12. **Melendi GA, Coviello S, Bhat N, Zea-Hernandez J, Ferolla FM, Polack FP.** 2010.  
416 Breastfeeding is associated with the production of type I interferon in infants infected with  
417 influenza virus. *Acta Paediatr* **99**:1517–1521.
- 418 13. **Scagnolari C, Midulla F, Pierangeli A, Moretti C, Bonci E, Berardi R, De Angelis D,**  
419 **Selvaggi C, Di Marco P, Girardi E, Antonelli G.** 2009. Gene expression of nucleic acid-  
420 sensing pattern recognition receptors in children hospitalized for respiratory syncytial virus-  
421 associated acute bronchiolitis. *Clin vaccine Immunol* **16**:816–23.
- 422 14. **Witte K, Witte E, Sabat R, Wolk K.** 2010. IL-28A, IL-28B, and IL-29: promising  
423 cytokines with type I interferon-like properties. *Cytokine Growth Factor Rev* **21**:237–51.
- 424 15. **Okabayashi T, Kojima T, Masaki T, Yokota S-I, Imaizumi T, Tsutsumi H, Himi T,**  
425 **Fujii N, Sawada N.** 2011. Type-III interferon, not type-I, is the predominant interferon  
426 induced by respiratory viruses in nasal epithelial cells. *Virus Res* **160**:360–6.
- 427 16. **Donnelly RP, Kotenko S V.** 2010. Interferon-Lambda: A New Addition to an Old Family.  
428 *J Interf Cytokine Res* **30**:555–564.
- 429 17. **Doyle SE, Schreckhise H, Khuu-Duong K, Henderson K, Rosler R, Storey H, Yao L,**  
430 **Liu H, Barahmand-pour F, Sivakumar P, Chan C, Birks C, Foster D, Clegg CH,**  
431 **Wietzke-Braun P, Mihm S, Klucher KM.** 2006. Interleukin-29 uses a type 1 interferon-  
432 like program to promote antiviral responses in human hepatocytes. *Hepatology* **44**:896–906.

- 433 18. **Haller O, Kochs G.** 2011. Human MxA protein: an interferon-induced dynamin-like  
434 GTPase with broad antiviral activity. *J Interf cytokine Res Off J Int Soc Interf Cytokine Res*  
435 **31:79–87.**
- 436 19. **Elliott J, Lynch OT, Suessmuth Y, Qian P, Boyd CR, Burrows JF, Buick R, Stevenson**  
437 **NJ, Touzelet O, Gadina M, Power UF, Johnston JA.** 2007. Respiratory syncytial virus  
438 NS1 protein degrades STAT2 by using the Elongin-Cullin E3 ligase. *J Virol* **81:3428–3436.**
- 439 20. **Ling Z, Tran KC, Teng MN.** 2009. Human respiratory syncytial virus nonstructural protein  
440 NS2 antagonizes the activation of beta interferon transcription by interacting with RIG-I. *J*  
441 *Virol* **83:3734–42.**
- 442 21. **Spann KM, Tran K-C, Chi B, Rabin RL, Collins PL.** 2004. Suppression of the induction  
443 of alpha, beta, and lambda interferons by the NS1 and NS2 proteins of human respiratory  
444 syncytial virus in human epithelial cells and macrophages [corrected]. *J Virol* **78:4363–9.**
- 445 22. **Touzelet O, Loukili N, Pelet T, Fairley D, Curran J, Power UF.** 2009. De novo  
446 generation of a non-segmented negative strand RNA virus with a bicistronic gene. *Virus Res*  
447 **140:40–48.**
- 448 23. **Villenave R, O'Donoghue D, Thavagnanam S, Touzelet O, Skibinski G, Heaney LG,**  
449 **McKague JP, Coyle P V, Shields MD, Power UF.** 2011. Differential cytopathogenesis of  
450 respiratory syncytial virus prototypic and clinical isolates in primary pediatric bronchial  
451 epithelial cells. *Virol J* **8:43.**

- 452 24. **Techaarpornkul S, Barretto N, Peeples ME.** 2001. Functional analysis of recombinant  
453 respiratory syncytial virus deletion mutants lacking the small hydrophobic and/or  
454 attachment glycoprotein gene. *J Virol* **75**:6825–34.
- 455 25. **Collins PL, Hill MG, Camargo E, Grosfeld H, Chanock RM, Murphy BR.** 1995.  
456 Production of infectious human respiratory syncytial virus from cloned cDNA confirms an  
457 essential role for the transcription elongation factor from the 5' proximal open reading frame  
458 of the M2 mRNA in gene expression and provides a capability for vaccine . *Proc Natl Acad*  
459 *Sci U S A* **92**:11563–7.
- 460 26. **Webster Marketon JI, Corry J, Teng MN.** 2014. The respiratory syncytial virus (RSV)  
461 nonstructural proteins mediate RSV suppression of glucocorticoid receptor transactivation.  
462 *Virology* **449**:62–9.
- 463 27. **Power UF, Plotnicky-Gilquin H, Huss T, Robert A, Trudel M, Stahl S, Uhlen M,**  
464 **Nguyen TN, Binz H.** 1997. Induction of protective immunity in rodents by vaccination with  
465 a prokaryotically expressed recombinant fusion protein containing a respiratory syncytial  
466 virus G protein fragment. *Virology* **230**:155–166.
- 467 28. **Villenave R, Touzelet O, Thavagnanam S, Sarlang S, Parker J, Skibinski G, Heaney**  
468 **LG, McKaigue JP, Coyle P V, Shields MD, Power UF.** 2010. Cytopathogenesis of Sendai  
469 virus in well-differentiated primary pediatric bronchial epithelial cells. *J Virol* **84**:11718–  
470 28.

- 471 29. **Heaney LG, Stevenson EC, Turner G, Cadden IS, Taylor R, Shields MD, Ennis M.**  
472 1996. Investigating paediatric airways by non-bronchoscopic lavage: normal cellular data.  
473 Clin Exp Allergy **26**:799–806.
- 474 30. **Coyle P V, Ong GM, O’Neill HJ, McCaughey C, Ornellas D De, Mitchell F, Mitchell**  
475 **SJ, Feeney SA, Wyatt DE, Forde M, Stockton J.** 2004. A touchdown nucleic acid  
476 amplification protocol as an alternative to culture backup for immunofluorescence in the  
477 routine diagnosis of acute viral respiratory tract infections. BMC Microbiol **4**:41.
- 478 31. **Bousse T, Chambers RL, Scroggs RA, Portner A, Takimoto T.** 2006. Human  
479 parainfluenza virus type 1 but not Sendai virus replicates in human respiratory cells despite  
480 IFN treatment. Virus Res **121**:23–32.
- 481 32. **Taylor CE, Webb MS, Milner AD, Milner PD, Morgan L a, Scott R, Stokes GM,**  
482 **Swarbrick a S, Toms GL.** 1989. Interferon alfa, infectious virus, and virus antigen secretion  
483 in respiratory syncytial virus infections of graded severity. Arch Dis Child **64**:1656–60.
- 484 33. **Lo MS, Brazas RM, Holtzman MJ.** 2005. Respiratory syncytial virus nonstructural  
485 proteins NS1 and NS2 mediate inhibition of Stat2 expression and alpha/beta interferon  
486 responsiveness. J Virol **79**:9315–9.
- 487 34. **Jin H, Zhou H, Cheng X, Tang R, Munoz M, Nguyen N.** 2000. Recombinant respiratory  
488 syncytial viruses with deletions in the NS1, NS2, SH, and M2-2 genes are attenuated in vitro  
489 and in vivo. Virology **273**:210–8.



- 490 35. **Stoltz M, Klingström J.** 2010. Alpha/beta interferon (IFN-alpha/beta)-independent  
491 induction of IFN-lambda1 (interleukin-29) in response to Hantaan virus infection. *J Virol*  
492 **84**:9140–8.
- 493 36. **Holzinger D, Jorns C, Stertz S, Boisson-Dupuis S, Thimme R, Weidmann M, Casanova**  
494 **J-L, Haller O, Kochs G.** 2007. Induction of MxA gene expression by influenza A virus  
495 requires type I or type III interferon signaling. *J Virol* **81**:7776–85.
- 496 37. **Ramaswamy M, Shi L, Varga SM, Barik S, Behlke MA, Look DC.** 2006. Respiratory  
497 syncytial virus nonstructural protein 2 specifically inhibits type I interferon signal  
498 transduction. *Virology* **344**:328–39.
- 499 38. **Takeuchi O, Akira S.** 2009. Innate immunity to virus infection. *Immunol Rev* **227**:75–86.
- 500 39. **Kawai T, Akira S.** 2006. Innate immune recognition of viral infection. *Nat Immunol* **7**:131–  
501 7.
- 502 40. **Ren J, Liu T, Pang L, Li K, Garofalo RP, Casola A, Bao X.** 2011. A novel mechanism  
503 for the inhibition of interferon regulatory factor-3-dependent gene expression by human  
504 respiratory syncytial virus NS1 protein. *J Gen Virol* **92**:2153–9.
- 505 41. **Spann KM, Tran KC, Collins PL.** 2005. Effects of nonstructural proteins NS1 and NS2 of  
506 human respiratory syncytial virus on interferon regulatory factor 3, NF-kappaB, and  
507 proinflammatory cytokines. *J Virol* **79**:5353–62.

- 508 42. **Swedan S, Musiyenko A, Barik S.** 2009. Respiratory syncytial virus nonstructural proteins  
509 decrease levels of multiple members of the cellular interferon pathways. *J Virol* **83**:9682–  
510 9693.
- 511 43. **Killip MJ, Young DF, Ross CS, Chen S, Goodbourn S, Randall RE.** 2011. Failure to  
512 activate the IFN- $\beta$  promoter by a paramyxovirus lacking an interferon antagonist. *Virology*  
513 **415**:39–46.
- 514 44. **Brand S, Beigel F, Olszak T, Zitzmann K, Eichhorst ST, Otte J-M, Diebold J,**  
515 **Diepolder H, Adler B, Auernhammer CJ, Göke B, Dambacher J.** 2005. IL-28A and IL-  
516 29 mediate antiproliferative and antiviral signals in intestinal epithelial cells and murine  
517 CMV infection increases colonic IL-28A expression. *Am J Physiol Gastrointest Liver*  
518 *Physiol* **289**:G960–8.
- 519 45. **Sommereyns C, Paul S, Staeheli P, Michiels T.** 2008. IFN-lambda (IFN-lambda) is  
520 expressed in a tissue-dependent fashion and primarily acts on epithelial cells in vivo. *PLoS*  
521 *Pathog* **4**:e1000017.
- 522 46. **Donnelly RP, Dickensheets H, O'Brien TR.** 2011. Interferon-lambda and therapy for  
523 chronic hepatitis C virus infection. *Trends Immunol* **32**:443–50.
- 524 47. **Larkin J, Jin L, Farmen M, Venable D, Huang Y, Tan S-L, Glass JI.** 2003. Synergistic  
525 antiviral activity of human interferon combinations in the hepatitis C virus replicon system.  
526 *J Interferon Cytokine Res* **23**:247–57.
- 527 48. **Sainz B, Halford WP.** 2002. Alpha/Beta interferon and gamma interferon synergize to  
528 inhibit the replication of herpes simplex virus type 1. *J Virol* **76**:11541–50.

- 529 49. **Scagnolari C, Trombetti S, Alberelli A, Cicetti S, Bellarosa D, Longo R, Spanò A, Riva**  
530 **E, Clementi M, Antonelli G.** 2007. The synergistic interaction of interferon types I and II  
531 leads to marked reduction in severe acute respiratory syndrome-associated coronavirus  
532 replication and increase in the expression of mRNAs for interferon-induced proteins.  
533 *Intervirology* **50**:156–60.
- 534 50. **Huguenin A, Moutte L, Renois F, Leveque N, Talmud D, Abely M, Nguyen Y, Carrat**  
535 **F, Andreoletti L.** 2012. Broad respiratory virus detection in infants hospitalized for  
536 bronchiolitis by use of a multiplex RT-PCR DNA microarray system. *J Med Virol* **84**:979–  
537 85.
- 538 51. **Richard N, Komurian-Pradel F, Javouhey E, Perret M, Rajoharison A, Bagnaud A,**  
539 **Billaud G, Vernet G, Lina B, Floret D, Paranhos-Baccalà G.** 2008. The impact of dual  
540 viral infection in infants admitted to a pediatric intensive care unit associated with severe  
541 bronchiolitis. *Pediatr Infect Dis J* **27**:213–7.
- 542 52. **Martin ET, Kuypers J, Wald A, Englund J a.** 2012. Multiple versus single virus  
543 respiratory infections: viral load and clinical disease severity in hospitalized children.  
544 *Influenza Other Respi Viruses* **6**:71–7.

545

546

547 **Figure Legends.**

548 **Figure 1. Pre-infection of WD-PBECs with RSV induces an anti-viral effect.** WD-PBECs (n =  
549 3 donors) were mock-infected or infected with RSV BT2a (MOI~4). Seventy two hpi, RSV- and  
550 mock-infected cultures were super-infected with rSeV/eGFP (MOI~0.1). (A) RSV-infected and  
551 mock-infected cultures were monitored by UV microscopy every 24 h (original magnification, x4).  
552 These photos are representative of duplicate cultures from 3 individual donors. (B) eGFP  
553 expression was quantified every 24 h by measuring the % of green pixels in 3 different microscope  
554 fields. (C) Virus growth kinetics was determined by titrating rSeV/eGFP in apical washes at 24 h  
555 intervals following infection. Data are presented as mean  $\pm$  SEM log<sub>10</sub> fluorescent focus units  
556 (ffu)/mL.

557 **Figure 2. Type III IFN, but not type I IFN, is detected following RSV infection *in-vivo* and *in-***  
558 ***vitro*.** Lower airway samples from infants hospitalized for severe RSV infection (n=10 donors) and  
559 healthy controls (n=14 donors) were analyzed for pan-IFN- $\alpha$  (A), IFN- $\beta$  (B), IL-29 (C) or IL-28A  
560 (D) by ELISA. Data are presented as mean  $\pm$  SEM. Statistical analyses were undertaken using a  
561 non-parametric t-test followed by a Mann-Whitney test. \*\*\*p = 0.0005. WD-PBECs (n=5 donors)  
562 were infected with RSV (MOI~4). IL-29 (E) or IL-28A (F) secretions in the basolateral medium  
563 of RSV- and mock-infected cultures harvested at 24 and 96 hpi were measured. As the medium  
564 was replaced every day, the data correspond to IFN secretions within the preceding 24 h. Values  
565 are means  $\pm$  SEM. \*\*p<0.01.

566 **Figure 3. RSV-induced antiviral effect is partially mediated by IL-29.** WD-PBECs (n=2-4  
567 donors) were infected with RSV BT2a (MOI~4) or mock infected. Seventy two hpi, the basal  
568 medium of mock- (CM<sub>CON</sub>) or RSV-infected cultures incubated with (CM<sub>RSV</sub> +  $\alpha$ IL-29) or without

569 (CM<sub>RSV</sub>) neutralizing antibody against IL-29 (10 µg/mL) was transferred into the basal  
570 compartment of fresh cultures from the same individual donor. Twenty four h later, the cultures  
571 were infected with rSeV/eGFP (MOI~0.1). (A) eGFP expression in CM<sub>CON</sub>-, CM<sub>RSV</sub> + αIL-29-  
572 and CM<sub>RSV</sub>-treated rSeV/eGFP-infected WD-PBECs over time (original magnification x4). (B)  
573 eGFP expression was quantified every 24 h by measuring the % green pixels in 5 random  
574 microscopic fields. (C) Virus growth kinetics were determined by titrating rSeV/eGFP in apical  
575 washes at 24 h intervals following infection. Data are presented as mean ± SEM log<sub>10</sub> ffu/mL. Area  
576 under the curves were calculated and compared using an unpaired Student's t-test. \*\*p < 0.01; \*\*\*p  
577 < 0.001.

578 **Figure 4. Influence of IL-29 pre-treatment on rSeV/eGFP growth in WD-PBECs.** WD-PBECs  
579 (n=3 donors) were pre-treated with IL-29 (100 pg/mL and 1000 pg/mL) or mock-treated. Twenty  
580 four h later, cultures were infected with rSeV/eGFP at an MOI~0.1. UV microphotographs were  
581 taken every 24 hpi (A). Original magnification, x4. eGFP expression was quantified every 24 hpi  
582 by measuring the % green pixels in 3 random microscopic fields (B). Virus growth kinetics were  
583 determined by titrating rSeV/eGFP in apical washes at 24 h intervals following infection (C). Data  
584 are presented as mean ± SEM log<sub>10</sub> ffu/mL. Area under the curves were calculated and compared  
585 using an unpaired Student's t-test. \*p<0.05.

586 **Figure 5. CM<sub>RSV</sub> and IL-29 pre-treatment attenuates RSV growth in WD-PBECs.** WD-  
587 PBECs (n=2 donors) were infected in duplicate with RSV BT2a (MOI~4) or mock infected.  
588 Seventy two hpi, the basal medium of mock- (CM<sub>CON</sub>) or RSV-infected cultures (CM<sub>RSV</sub>) was  
589 transferred into the basal compartment of fresh cultures from the same individual donor. Twenty  
590 four h later, the cultures were infected with rA2-eGFP (MOI~0.1). eGFP expression was quantified  
591 every 24 h by measuring the % green pixels in 3 different microscopic fields (A). Virus growth

592 kinetics were determined by titrating rA2-eGFP in apical washes at 24 h intervals following  
593 infection (B). WD-PBECs (n=2-3 donors) were pre-treated with IL-29 (1 or 100 ng/mL). Twenty  
594 four h later, cultures were infected with RSV BT2a at an MOI~0.01 (C). WD-PBECs (n=3 donors)  
595 were infected with RSV BT2a at an MOI of 0.01. Two or 24 hpi, infected cultures were treated  
596 with IL-29 (100 ng/mL) (D). Virus growth kinetics was determined by titrating RSV in apical  
597 washes every 24 h following infection for (C) and (D). Data are presented as mean + SEM log<sub>10</sub>  
598 TCID<sub>50</sub>/mL. Area under the curves were calculated and compared using an unpaired Student's t-  
599 test. \*p < 0.05, \*\*p < 0.01.

600 **Figure 6. rA2-ΔNS1/2-eGFP does not infect efficiently WD-PBECs.** WD-PBEC cultures were  
601 infected in duplicate with either rA2-eGFP or rA2-ΔNS1/2-eGFP (MOI~1) for 96 h. Representative  
602 fluorescence pictures were taken at 96 hpi (A). rA2-eGFP or rA2-ΔNS1/2-eGFP titers at 96 hpi  
603 were measured (B). Data are presented as mean ± SEM log<sub>10</sub>TCID<sub>50</sub>/mL. \*\*\* p < 0.001.

604 **Figure 7. RSV NS1/2 partially counteract IL-29-mediated anti-viral effects.** Vero cells were  
605 pre-treated with IL-29 (1 or 100 ng/mL) or non-treated. Twenty four h post treatment, the cells  
606 were infected with rA2-eGFP (A) or rA2-ΔNS1/2-eGFP (B) (MOI=0.1). Cultures were monitored  
607 by UV microscopy every 24 hpi (original magnification, x4). Infections were undertaken in  
608 triplicate and a surrogate for virus replication kinetics was quantified by measuring % eGFP  
609 coverage of 3-5 microscope fields at each time point (C, D). Data are presented as mean ± SEM  
610 eGFP area (% whole image) and are representative of three independent experiments in triplicate.  
611 Area under the curves were calculated and compared using an unpaired Student's t-test. \*\*\*p <  
612 0.001..

613 **Figure 8. MxA/B expression is induced following RSV infection, and IL-29 or CM<sub>RSV</sub>**  
614 **treatment of WD-PBECs.** (A) WD-PBECs were either mock-infected, RSV BT2a-infected (MOI  
615 ~0.1) for 96 h, or treated with IL-29 (1 ng/mL) for 24 h. Cultures were fixed and stained for MxA/B  
616 (red) and nuclei were counter-stained with DAPI (blue). Confocal images show typical staining in  
617 WD-PBECs from 3 individual donors. (original magnification, x63). (B) and (C) MxA/B  
618 expression following treatment with CM<sub>RSV</sub> is mediated in large part by IL-29. WD-PBECs (2  
619 independent cultures from 1 donor) were incubated with either CM<sub>RSV</sub> or CM<sub>CON</sub> alone or  
620 combined with a neutralizing antibody against IL-29 (10 µg/mL) for 24 h. Cultures were fixed and  
621 stained for MxA/B and nuclei were counter-stained with DAPI. The MxA/B signal was quantified  
622 in 5 individual fields from each culture, and mean fluorescence was calculated and plotted.  
623 \*\*p<0.01, \*\*\*p<0.001.

624 **Figure 9. RSV blocks the expression of MxA/B, p-STAT2 but not p-STAT1 in infected WD-**  
625 **PBECs.** WD-PBECs were either mock- or RSV-infected (MOI~0.1) for 96 h. Cultures were fixed  
626 and either stained for (A) MxA/B, (C) p-STAT1 or (E) p-STAT2 (red); RSV was detected using a  
627 FITC-conjugated anti-RSV-F-specific antibody (green). Confocal images show typical staining  
628 from WD-PBECs derived from 3 different individual donors (original magnification, x63).  
629 Fluorescence of MxA/B (B), p-STAT1 (D) and p-STAT2 (F) in RSV-infected and uninfected cells  
630 within RSV-infected WD-PBEC cultures was quantified by dividing the Raw Integrated Density  
631 by the Area of >120 individual cells. Fluorescence was quantified using ImageJ software. Data are  
632 presented as mean ± SEM. \*\*\*p < 0.0005.

633

634

# Fig.1

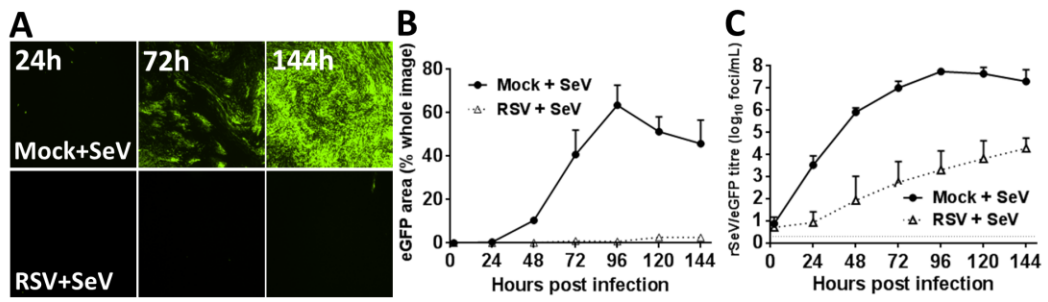
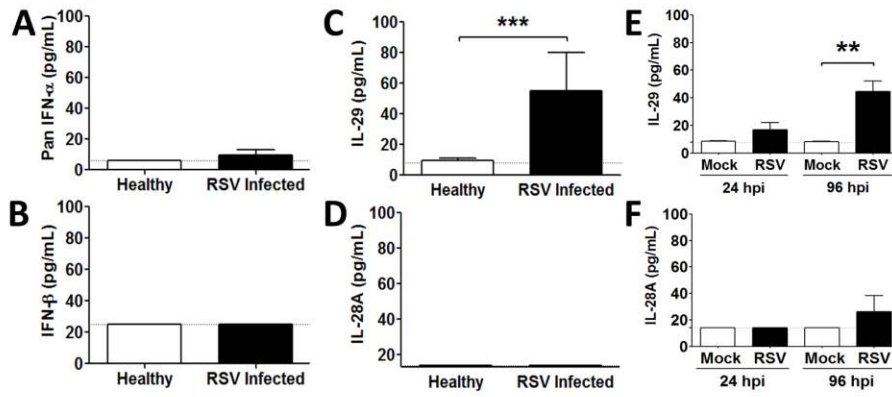
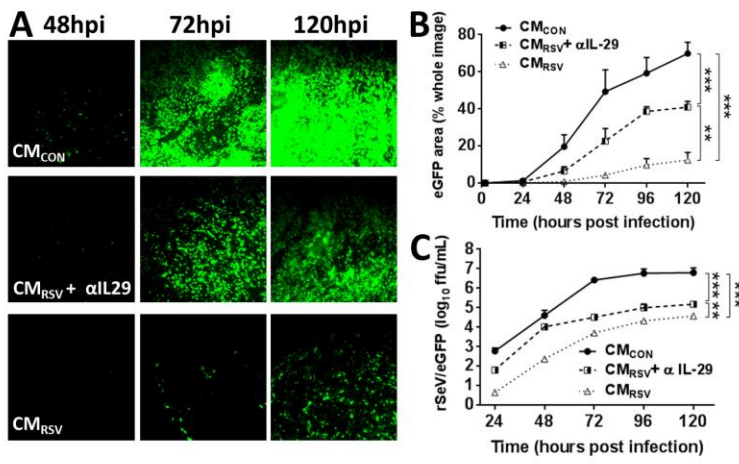




Fig.2



# Fig.3



# Fig. 4

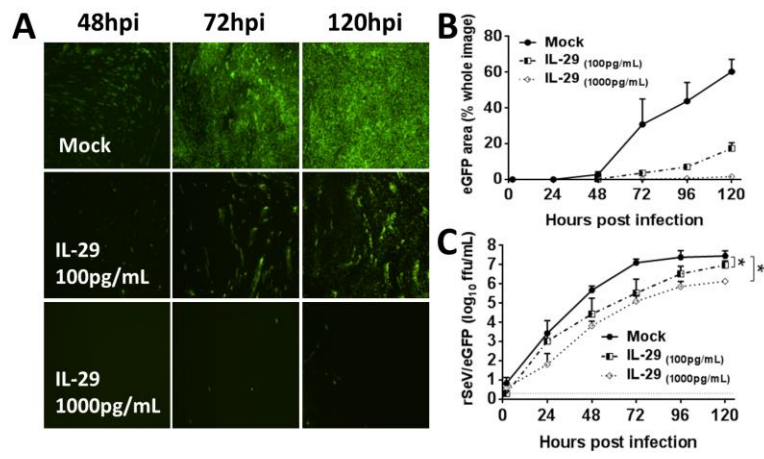


# Fig. 5

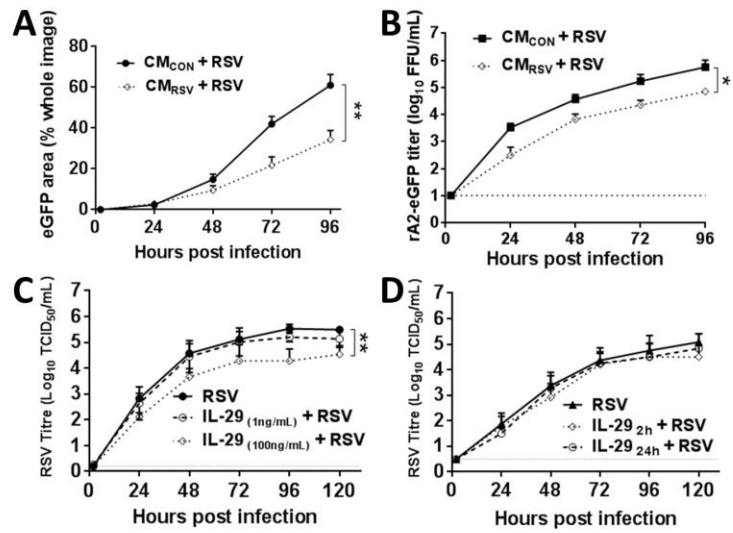


# Fig.6

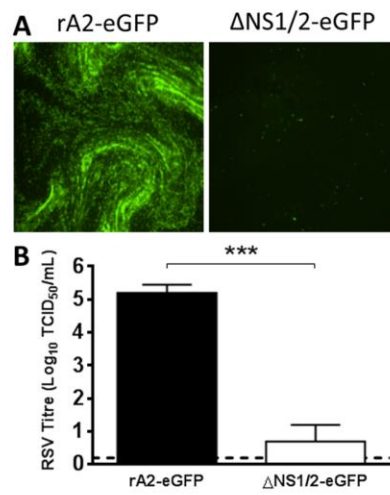


# Fig. 7

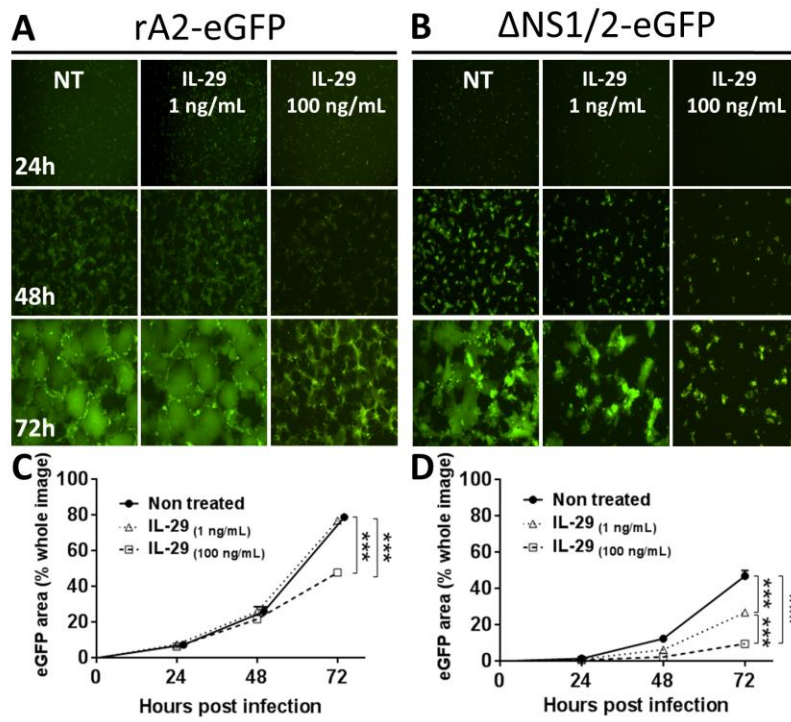


# Fig.8

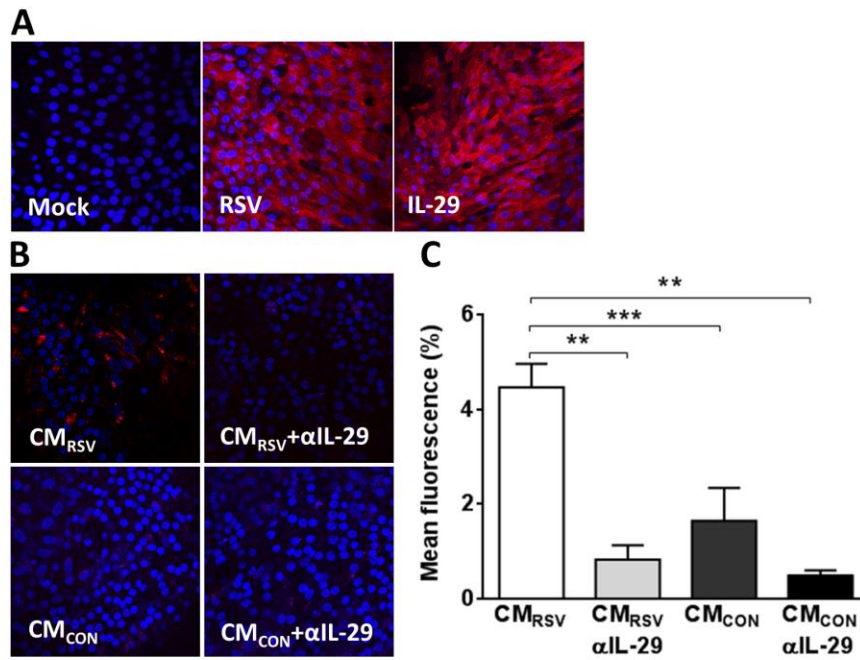


# Fig.9

